International Journal of Cardiology 274 (2019) 271–278

Contents lists available at ScienceDirect

International Journal of Cardiology

journal homepage: www.elsevier.com/locate/ijcard

Hyperbaric oxygen boosts long noncoding RNA MALAT1 exosome secretion to suppress microRNA-92a expression in therapeutic angiogenesis

Kou-Gi Shyu [a], Bao-Wei Wang [b], Chun-Ming Pan [b], Wei-Jen Fang [b], Chiu-Mei Lin [c,d,*,1]

[a] Division of Cardiology, Shin Kong Wu Ho-Su Memorial Hospital, Taipei, Taiwan
[b] Department of Medical Education and Research, Shin Kong Wu Ho-Su Memorial Hospital, Taipei, Taiwan
[c] Department of Emergency Medicine, Shin Kong Wu Ho-Su Memorial Hospital, Taipei, Taiwan
[d] School of Medicine, Fu-Jen Catholic University, New Taipei City, Taiwan

ARTICLE INFO

Article history:
Received 17 May 2018
Received in revised form 21 September 2018
Accepted 28 September 2018
Available online 2 October 2018

Keywords:
Hyperbaric oxygen
MALAT1
Coronary artery endothelial cells
microRNA-92a
Exosome

ABSTRACT

Background: Hyperbaric oxygen (HBO) could improve wound healing by enhancement of angiogenesis. The effect of HBO on metastasis-associated lung adenocarcinoma transcript 1 (MALAT1), a proangiogenic long non-coding RNA, and on endothelial cell-derived exosome is unknown. We aim to investigate both whether MALAT1 is altered in human coronary artery endothelial cells (HCAECs)-derived exosomes in response to HBO as well as the molecular regulatory mechanisms of MALAT1 in HCAECs under HBO treatment.

Methods and results: HCAECs were cultured and HBO was applied at 2.5 atmosphere absolute (ATA) in a hyperbaric chamber. Exosomes were extracted from culture media. A rat model of hind-limb ischemia was performed by ligation of the right femoral artery. HBO at 2.5 ATA significantly increased MALAT1 expression in HCAECs and HCAECs-derived exosomes. MALAT1 suppressed miR-92a expression in HCAEC-derived exosomes under HBO. Silencing MALAT1 by MALAT1 siRNA significantly inhibited KLF2 mRNA expression induced by HBO, as did MiR-92a. MiR-92a significantly decreased KLF2 luciferase activity in HCAECs under HBO. HBO and HBO-induced exosomes significantly increased cell proliferation and the capillary-like network formation of HCAECs. MALAT1 siRNA and miR-92a overexpression significantly attenuated the cell proliferation and tube formation caused by HBO-induced exosome. HBO and HBO-induced exosomes significantly improved neovascularization in a rat model of hind-limb ischemia.

Conclusions: HBO upregulates MALAT1 to suppress miR-92a expression and counteracts the inhibitory effect of miR-92a on KLF2 expression in HCAECs to enhance neovascularization. HBO-induced derivation of exosomes from HCAECs enhances angiogenesis. Exosomes containing MALAT1 might serve as a valuable therapeutic tool for neovascularization by HBO.

1. Introduction

Hyperbaric oxygen (HBO) therapy has been used for decades to treat various clinical conditions [1] because it significantly increases the oxygen content in hypoperfused tissues, and the elevated oxygen content in hypoxic tissues enhances the ischemic repair process [2,3]. One of the mechanisms through which HBO therapy promotes wound healing is the enhancement of neovascularization in the ischemic tissue [4].

Long noncoding RNAs (lncRNA), a type of noncoding RNAs with a length >200 nucleotides, can regulate gene expression at epigenetic, transcriptional, and posttranscriptional levels and play a vital role in the prevention of cardiovascular diseases [5]. An endothelial-enriched lncRNA, metastasis-associated lung adenocarcinoma transcript 1 (MALAT1), was reported to regulate endothelial cell function and vessel growth because loss of MALAT1 impaired neovascularization in vitro and in vivo [6]. More recently, MALAT1 has been reported to play a role in the promotion of angiogenesis by mesenchymal stem cells in thyroid tumors [7,8]. These data indicate that MALAT1 can be considered a proangiogenic lncRNA. However, no data have been presented to verify the effect of HBO therapy on the regulation of MALAT1 in human coronary artery endothelial cells (HCAECs). Therefore, we hypothesized that HBO can potentially affect the expression

Abbreviations: ATA, atmosphere absolute; HCAECs, human coronary artery endothelial cells; HBO, hyperbaric oxygen; siRNAs, small interfering RNAs; LNA, locked nucleic acid; KLF2, Kruppel-like factor 2; lncRNAs, long non-coding RNAs; MALAT1, metastasis-associated lung adenocarcinoma transcript 1; miR, microRNA; PCR, polymerase chain reaction; RT, reverse transcription.

* Corresponding author at: Department of Emergency Medicine, Shin Kong Wu Ho-Su Memorial Hospital, No. 95 Wen-Chang Rd, Shih Lin District, Taipei 111, Taiwan.
E-mail address: mei882153@gmail.com (C.-M. Lin).

[1] The author takes responsibility for all aspects regarding the reliability and freedom from bias of the data presented and their discussed interpretation.

https://doi.org/10.1016/j.ijcard.2018.09.118

of MALAT1 in HCAECs and investigated the molecular regulatory mechanisms of MALAT1 in HCAECs under HBO treatment.

Exosomes are extracellular vesicles of the endosomal origin that play a vital role in intercellular functions [9]. Exosomes are considered as emerging diagnostic markers with cell-free therapeutic potential in the treatment of cardiovascular diseases [9,10]. Endothelial cells release exosomes that may contain both autocrine and paracrine angiogenic factors [11,12]. The effect of HBO on endothelial-cell–derived exosomes remains unclear.

2. Materials and methods

2.1. Primary human coronary artery endothelial cell culture

HCAECs were purchased from PromoCell GmbH (Heidelberg, Germany). The cells were cultured in an endothelial cell growth medium, MV, supplemented with 10% fetal bovine serum, 100 U/mL of penicillin, and 100 μg/mL of streptomycin at 37 °C in a humidified atmosphere of 5% CO_2. Cells were grown to an 80%–90% confluence in 15-cm culture dishes and were subcultured at a ratio of 1:3. For exosome collection, 10 mL of the cell-free supernatant was collected from the HCAEC culture after increasing the amount of HBO.

2.2. HBO treatment

For HBO treatment, HCAECs were exposed to different degrees of atmosphere absolute (ATA) of oxygen (95% oxygen, 3% air, and 2% carbon dioxide) in a hyperbaric chamber for 1 h/day, and HBO at 2.5 ATA was applied at 1 h/day for 1 to 7 days. The small hyperbaric chamber was placed in a temperature-controlled (37 °C) incubator, as described previously [13].

2.3. Extraction of exosomes from cell media

Exosomes were isolated from cell culture media using a total exosome isolation reagent (Invitrogen, Thermo Fisher Scientific, MA, USA) according to manufacturer's instructions. Briefly, the cell-free supernatant was centrifuged at 2000*g* for 30 min to remove cell debris. The supernatant containing cell-free cell media was transferred to a fresh container and held on ice until use. Each sample was combined with half volume of the total exosome isolation reagent and mixed well by vortexing or pipetting up and down until a homogenous solution formed. The samples were incubated overnight at 4 °C and then centrifuged at 4 °C at 10,000*g* for 1 h. The supernatant was aspirated and discarded, and the exosome pellet was resuspended in 1× phosphate buffered saline (PBS) buffer and then stored at 4 °C for the short term (1–7 days) or −20 °C for the long term. The exosome was quantitated using an ExoQuant™ quantification assay kit according to manufacturer's instructions (BioVision, Milpitas, CA, USA).

2.4. RNA quality assessment of exosome

The RNA quality assessment of exosomes was performed using the Agilent 2100 Bioanalyzer with an RNA Pico chip (Agilent Technologies, Waldbronn, Germany) in accordance with manufacturer's instructions. For visualization and better interpretation, an electropherogram and a virtual gel image were generated (Supplemental Fig. I). All assessments were performed in duplicates.

2.5. Western blot analysis

HCAECs treated with HBO were harvested by scraping and then centrifuging (300 ×g) for 10 min at 4 °C. The proteins of interest were identified through treatment with specific antibodies, as indicated (1:1000 dilution), for 1 h at room temperature. Equal protein loading of the samples was further verified by staining the mouse antitubulin monoclonal antibody from Santa Cruz Biotechnology Inc. The procedure was performed as previously described [13].

2.6. Reverse transcription and real-time quantitative polymerase chain reaction

To quantify MALAT1-exosome mRNA transcripts, 12 μL of a 14-μL RNA eluate was subjected to reverse transcription (RT) with random hexamers using high-capacity cDNA reverse transcription kits (Applied biosystems, Thermo Fisher Scientific, MA, USA). Primers used for MALAT1 and miR92a were purchased from Thermo Fisher Scientific, MA, USA with Assay IDs Hs00273907_s1 and 000431, respectively. Primers used for Kruppel-like factor 2 (KLF2) were 5′-AAGGGCCTTTGTACTG-3′ (forward) and 5′-ATAAAA ACGAACCAGGTAGC-3′ (reverse). Primers used for α-tubulin were 5′-GATCACCAATGCTT GCTTTGAG-3′ (forward) and 5′-ACCATGGCGAGGGTCACAT-3′ (reverse). The procedure was performed as previously described [13].

2.7. Transfection of siRNAs or locked nucleic acid GapmeR

HCAECs were transfected at a confluence of 60%–75% with 50 nmol/L of synthesized small interfering RNAs (Ambion, Thermo Fisher Scientific, MA, USA) or 25 nmol/L of locked nucleic acid (LNA) GapmeR (Product No. 300630-101, Exiqon, Vedbaek, Denmark) targeting MALAT1 by using Lipofectamine RNAiMax (Invitrogen, Thermo Fisher Scientific, MA, USA) according to the manufacturer's protocol. The sequences of siRNA for MALAT1 were as follows: sense, GAGCUUGACUUGAUUGUAUtt, and antisense, AUACAAUCAAGUCAAGCUCct. For the negative control, scramble siRNA or negative control LNA GapmeR was also transfected. Scramble siRNA was purchased from Ambion (Catalog #: 4390847, Ambion, Thermo Fisher Scientific, MA, USA). The sequence of the negative control LNA GapmeR was 5′-AACACGTCTATACGC-3′ (Exiqon, Vedbaek, Denmark).

2.8. Luciferase activity assay

A 500-bp human KLF2 3′-UTR DNA fragment was generated (Chromosome 19: 16,324,817-16,327,874; http://www.ensembl.org/index.html) through artificial synthesis and cloning into a pUC57 vector. The clone was digested with *Mlu*I and *Bgl*II restriction enzymes and ligated into a pGL3-basic luciferase plasmid vector. The KLF2 3′-UTR contained miR-92a conserved sites at 3′-UTR (from 242 to 249 bp). For the mutant, the conserved site GTGCAATA was mutated into CACGTTAT and constructed using the same aforementioned method. All the cloned plasmids were confirmed through DNA sequencing (Seeing Bioscience Co. Ltd. Taipei, Taiwan). Plasmids were transfected into HCAECs by using a low-pressure accelerated gene gun (Bioware Technologies, Taipei, Taiwan) in accordance with the manufacturer's protocol. The test plasmid (2 μg) and the control plasmid (pGL4-Renilla luciferase, 0.02 μg) were cotransfected with the gene gun in each well and then replaced with a normal culture medium. Following various periods of HBO exposure, cell extracts were prepared using the dual-luciferase reporter assay system (Promega) and measured for dual-luciferase activity by using a luminometer (Glomax Multi Detection System, Promega, Madison, WI, USA).

2.9. Cell proliferation and viability assay

Cell proliferation and viability were measured using the CellTiter-Glo® luminescent cell viability assay kit (Promega Corporation, Madison, WI, USA) according to manufacturer's instructions. Briefly, HCAECs were grown and assayed in an HCAEC medium at 25,000 cells per well in a 96-well plate. After an equal volume of CellTiter-Glo® reagent was added, plates were shaken and then incubated at room temperature for 10 min to stabilize the luminescence signal. Finally, cell proliferation was quantified as the relative luminescence unit by using a luminometer (Glomax, Promega Corporation, Madison, WI, USA).

2.10. Capillary-like network formation assay

A capillary-like network formation was performed in an in vitro culture system. A 24-well culture plate was coated with 250 μL of Matrigel (BD Biosciences, MA), which was allowed to solidify (37 °C, 1 h). HCAECs were cultured on a Matrigel matrix and exposed to 2.5 ATA of oxygen (98% oxygen plus 2% CO_2) in a hyperbaric chamber for 5 h at 37 °C. After HBO treatment, cells were placed in a humidified incubator for 16 h at an atmosphere of 5% CO_2 at 37 °C. Exosomes extracted from 10 mL of the supernatant of cultured 6×10^6 HCAECs after HBO treatment were added to the cells in a humidified incubator for 16 h at an atmosphere of 5% CO_2 at 37 °C. The capillary-like network formation was observed using a phase-contrast microscope (Nikon, Tokyo). Tube formation with branching points was measured using Nikon NIS-Elements software (Nikon Imaging Japan Inc.).

2.11. Rat model of hind limb ischemia

Fifteen-week-old male Wistar rats, weighing 220–250 g, were kept under conventional conditions with free access to water and standard food. Animal experiments were approved and performed in accordance with the Guide for the Care and Use of Laboratory Animals published by the US National Institutes of Health (NIH Publication No. 85-23, revised 1996). After a fully anesthetized state (e.g., no response to toe pinching) had been confirmed following the induction of anesthesia with 2% isoflurane, the rats were subjected to hind limb ischemia through the ligation of the right femoral artery. In total, 70 μg of purified exosomes, 25 nM siRNA, or 40 μg of plasmid DNA was transfected into the ligation wound in the right femoral artery of the rats by using a low-pressure accelerated gene gun (Bioware Technologies, Taipei, Taiwan) following manufacturer's instructions. In brief, purified exosomes, siRNA, or plasmid DNA were suspended in 50 μL of PBS and added to the loading hole near the nozzle. Blood flow was assessed using a laser Doppler perfusion imager system (MoorLDI measurement version 5.3, Moor Instrument Ltd., England) 2 weeks after hind limb ischemia had been induced. Relative blood flow was determined as the ratio of blood flow to the ischemic limb to that to the nonischemic limb. For HBO treatment, the treated rats were exposed to 2.5 ATA of oxygen (95% oxygen, 3% air plus 2% carbon dioxide) in a hyperbaric chamber for 2 weeks, 1 h/per day at room temperature. This oxygen tension was selected based on current human treatment protocols [14].

2.12. Statistical analysis

The data are expressed as the mean ± SD. Statistical significance was ascertained using analysis of variance (ANOVA; GraphPad Software Inc., San Diego, CA). The Tukey–Kramer comparison test was used to conduct pairwise comparisons between multiple groups after ANOVA. A value of $P < 0.05$ was considered statistically significant.

3. Results

3.1. HBO increases MALAT1 expression in HCAEC and HCAEC-derived exosomes

To determine the effect of HBO on MALAT1 expression in HCAEC-derived exosomes, various ATAs of HBO were applied. As indicated in Fig. 1A, HBO caused a significant increase in MALAT1 from 1 to 3 ATA at 1 h/day for 2 days, with 2.5 ATA of HBO demonstrating the maximal effect on MALAT1 expression. Therefore, 2.5 ATA of HBO was used for the following experiments. HBO at 2.5 ATA significantly increased MALAT1 expression in HCAEC-derived exosomes from 1 to 3 days and then declined gradually to the control level at day 6 (Fig. 1B). The maximal effect of HBO at 2.5 ATA on MALAT1 expression occurred after 2 days of exposure. Similar to the effect of HCAEC-derived exosomes on MALAT1 expression, HBO alone at 2.5 ATA had the maximal effect on MALAT1 expression in HCAECs (Fig. 1C). HBO derived exosome treatment on HCAECs induced more significant MALAT1 expression than did exosomes without HBO treatment (Supplemental Fig. II). The exosome isolation through another method with a Qiagen-exoEasy maxi kit also demonstrated that HBO at 2.5 ATA significantly increased MALAT1 expression in HCAEC-derived exosomes from days 1 to 5 and then declined to the control level at day 6 (Supplemental Fig. III). We used a SYTO RNASelect Green Fluorescent Cell Stain to prove the existence of RNA in the exosomes. As presented in Supplemental Fig. IV, the green fluorescent stain signal increased in HCAECs with HBO-induced exosome treatment. We also used an in situ hybridization assay to demonstrate the increased expression of MALATI in HCAECs after HBO-derived exosome treatment, as indicated in Supplemental Fig. V. Furthermore, we demonstrated the presence of TSG101 as well as the characterization of exosomes derived from HCAECs both with and without HBO treatment, as displayed in Supplemental Fig. VI.

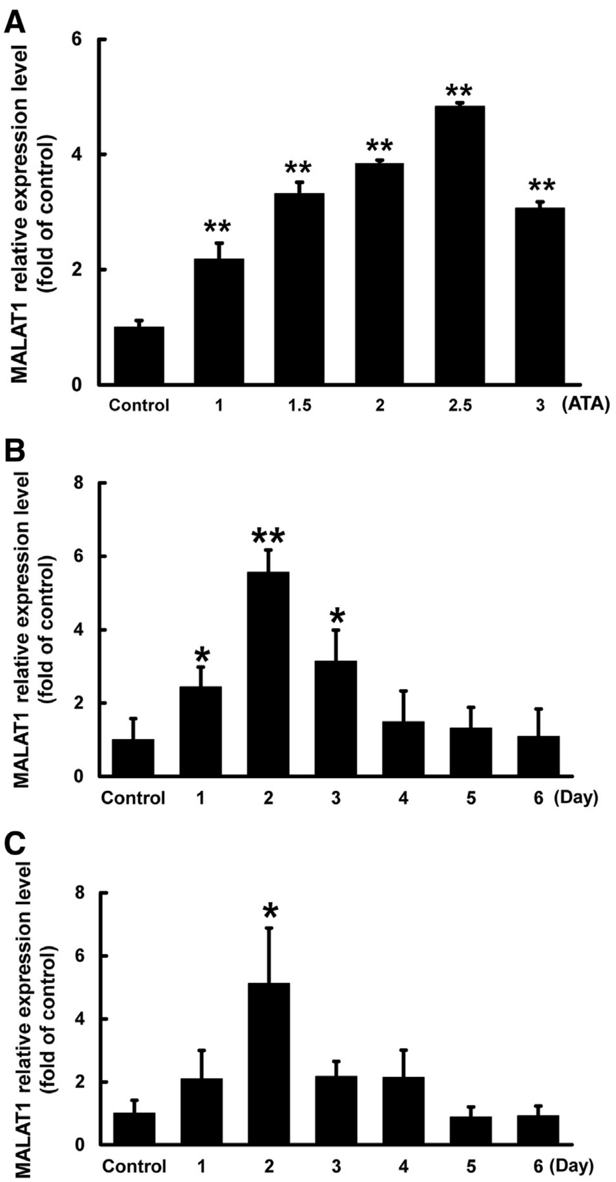

Fig. 1. Effect of HBO on HCAEC-derived exosomal MALAT1 expression. A. Quantitative real-time PCR of HCAEC-derived exosomal MALAT1 under various degrees of HBO for 2 days. The values from treated HCAECs are expressed as a ratio of normalized values of MALAT1 mRNA in the control cells. The Tukey–Kramer comparison test was conducted for statistical analysis. **$P < 0.01$ vs. control; $n = 4$ per group. B, Quantitative real-time PCR of HCAEC-derived exosomal MALAT1 under 2.5 ATA at 1 h each day for different durations. The values from treated HCAECs are expressed as a ratio of normalized values of MALAT1 mRNA in the control cells. The Tukey–Kramer comparison test was conducted for statistical analysis. *$P < 0.05$ vs. control. **$P < 0.01$ vs. control; $n = 5$ per group. C, Quantitative real-time PCR of HCAEC MALAT1 under 2.5 ATA at 1 h each day for different durations. The values from treated HCAECs are expressed as a ratio of normalized values of MALAT1 mRNA in the control cells. The Tukey–Kramer comparison test was conducted for statistical analysis. *$P < 0.01$ vs. control; $n = 4$ per group.

3.2. HBO decreases miR-92a expression in HCAEC-derived exosomes

We used the Clustal W method in MegAlign software (DNASTAR, Madison, WI, USA) to search for the target microRNA (miR) of MALAT1. We discovered that the sequences in miR-92a-3p were complementary to MALAT1 (sequence from 2345 to 2375). As indicated in the upper panel of Fig. 2A, HBO at 2.5 ATA significantly decreased miR-92a expression at three occasions of exposure. Inhibiting MALAT1 expression by using small interfering RNA could reverse miR-92a expression to reach the control level (Fig. 2B). Overexpression of wild type MALAT1 but not mutant MALAT1 significantly attenuated the miR-92a expression in HCAECs (Supplemental Fig. VII). This result indicated that MALAT1 suppresses miR-92a expression in HCAEC-derived exosomes under HBO treatment.

3.3. HBO increases KLF2 expression in HCAECs with MALAT1 and miR-92a

HBO at 2.5 ATA significantly increased KLF2 mRNA expression in HCAECs after 4 to 5 occasions of HBO exposure (1 h per day for each occasion) as presented in the upper panel of Fig. 2C. HBO at 2.5 ATA also significantly increased KLF2 protein expression after 5 occasions of HBO exposure (Fig. 2D and E). Silencing MALATA1 with MALAT1 siRNA significantly inhibited the KLF2 mRNA and protein expression induced by HBO (Fig. 3A, B, and C). MALAT1 scramble siRNA did not significantly affect the KLF2 mRNA and protein expression induced by HBO. Overexpression of wild-type miR-92a significantly inhibited the KLF2 mRNA and protein expression induced by HBO. MiR-92a antagomir significantly reversed the KLF2 expression induced by miR-92a overexpression. The overexpression of the miR-92a mutant did not significantly affect KLF2 expression. These results indicated that HBO increases MALAT1 expression but decreases miR-92a expression to enhance KLF2 expression in HCAECs.

3.4. miR-92a decreases KLF2 luciferase activity in HCAECs under HBO treatment

We discovered that KLF2 3′UTR (nucleotide from 228 to 249) had a binding site for miR-92a-3p, as indicated in Fig. 3D using the Clustal W method of the MegAlign software (DANSTAR, Madison, WI, USA). MiR-92a-3p overexpression could significantly decrease KLF2 luciferase activity in HCAECs under 2.5 ATA HBO treatment when miR-92a was bound to normal 3′UTR of KLF2 (Fig. 3E). The overexpression of mutant miR-92a-3p did not affect the luciferase activity, indicating that KLF2 is the target gene of miR92-3p.

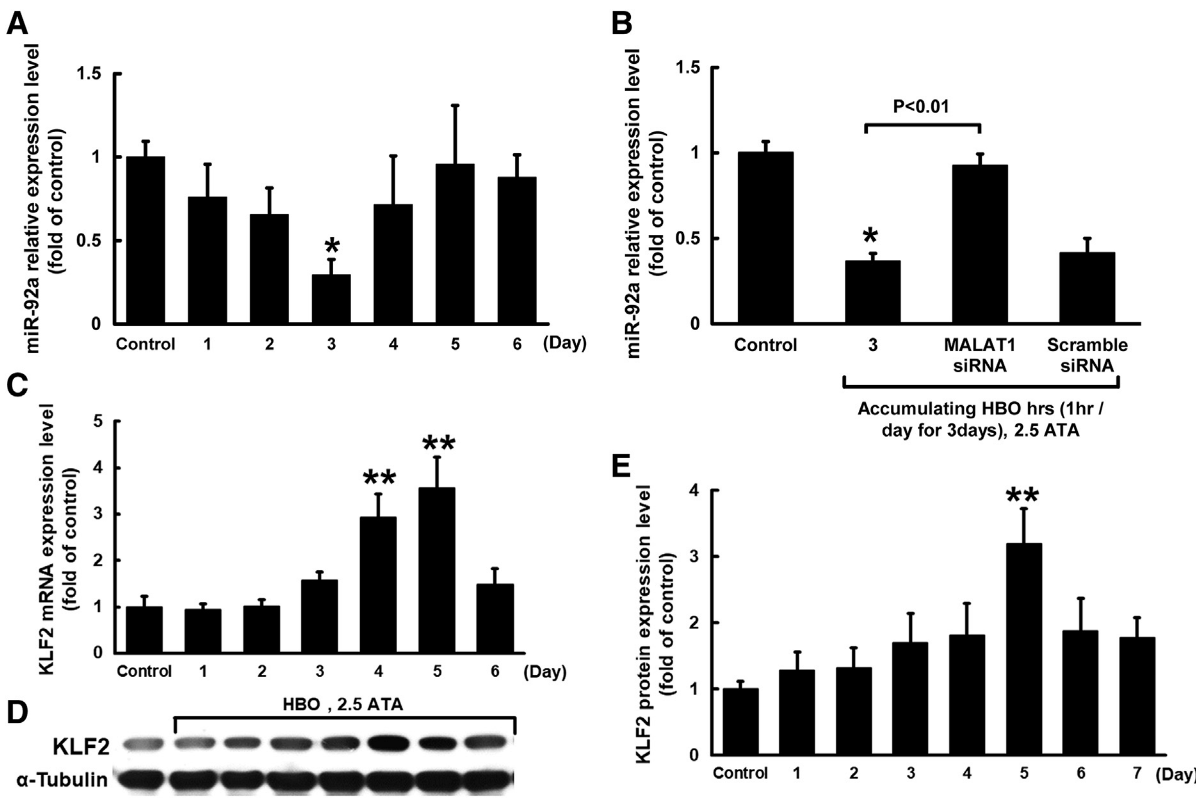

Fig. 2. Effect of HBO on miR-92a and KFL2 expression in HCAEC. A, Quantitative real-time PCR of HCAEC-derived exosomal miR-92a under 2.5 ATA at 1 h each day for different durations. The values from treated HCAECs are expressed as a ratio of normalized values of miR-92a mRNA in the control cells. The Tukey–Kramer comparison test was conducted for statistical analysis. *$P < 0.01$ vs. control; $n = 4$ per group. B, Quantitative real-time PCR of HCAEC-derived exosomal miR-92a under 2.5 ATA with or without MALAT1 siRNA treatment. The values from treated HCAECs are expressed as a ratio of normalized values of miR-92a mRNA in the control cells. Scramble siRNA is a control siRNA. The Tukey–Kramer comparison test was conducted for statistical analysis. *$P < 0.05$ vs. control; $n = 4$ per group. C, Quantitative real-time PCR of HCAEC KLF2 mRNA expression under 2.5 ATA at 1 h each day for different durations. The values from treated HCAECs are expressed as a ratio of normalized values of KLF2 mRNA in the control cells. The Tukey–Kramer comparison test was conducted for statistical analysis. **$P < 0.01$ vs. control; $n = 4$ per group. D, Representative Western blot. E, Quantitative analysis of KLF2 protein expression under 2.5 ATA at 1 h each day for different durations. The values from treated HCAEC groups were normalized to match α-tubulin measurements and then expressed as a ratio of normalized values to protein in the control group. The Tukey–Kramer comparison test was conducted for statistical analysis. **$P < 0.01$ vs. control; $n = 4$ per group.

3.5. HBO and HBO-induced exosomes increase HCAEC proliferation and viability

HBO for 5 h significantly increased the proliferation and viability of HCAECs in comparison with the control (Fig. 4A). HBO-induced exosomes from HCAECs also significantly increased cell proliferation and viability. Both pretreatment with MALAT1 siRNA and the overexpression of miR-92a significantly attenuated the proliferation and viability of HCAECs induced by exosomes. The scramble siRNA for MALAT1 and miR-92a antagomir did not inhibit the proliferation and viability induced by exosomes.

3.6. HBO and HBO-induced exosomes increased the capillary-like network formation of HCAECs with MALAT1 and miR-92a

HBO for 5 h significantly increased the tube formation of HCAECs (Fig. 4B and C). Both pretreatment with MALAT1 siRNA and the overexpression of miR-92a significantly blocked the tube formation from HBO. The scramble siRNA for MALAT1 and miR-92a antagomir did not inhibit HBO-induced tube formation. Exosomes extracted from HCAECS after HBO treatment for 5 h also significantly increased tube formation under typical cultured conditions without HBO treatment (Fig. 4D and E). Both pretreatment with MALAT1 siRNA and the overexpression of miR-92a significantly attenuated the exome-induced tube formation. The scramble siRNA for MALAT1 and miR-92a antagomir did not inhibit exome-induced tube formation.

3.7. HBO and HBO-induced exosomes increase blood flow in hind-limb ischemia

As presented in Fig. 4F and G, ligation of the right femoral artery of an adult rat impaired the blood flow to the ischemic hind-limb. HBO for 2 weeks and HBO-induced exosomes from HCAECs significantly improved blood flow to the ischemic hind-limb. Both pretreatment with MALAT1 siRNA and the overexpression of miR-92a significantly attenuated the ratio of HBO-induced blood flow. The scramble siRNA for MALAT1 and miR-92a antagomir did not attenuate the ratio of HBO-induced blood flow.

4. Discussion

The modulation of angiogenic MALAT1 responses might establish a link between angiogenesis and ischemic cardiovascular diseases. Indeed, lncRNA MALAT1 has been demonstrated to be capable of predicting metastasis and poor prognosis in patients with cancer [15]. In the vascular system, endothelial-expressed MALAT1 can regulate vessel growth and function [16]. Sun et al. reported that knockdown of MALAT1 expression could inhibit the proliferation of human umbilical-vein endothelial cells, a crucial component of angiogenesis [17]. Furthermore, MALAT1 was demonstrated to be significantly upregulated in the cardiac tissue of diabetic rats, partly through the inhibition of cardiomyocyte apoptosis [18]. In this study, we discovered that HBO significantly increased MALAT1 expression in HCAECs and

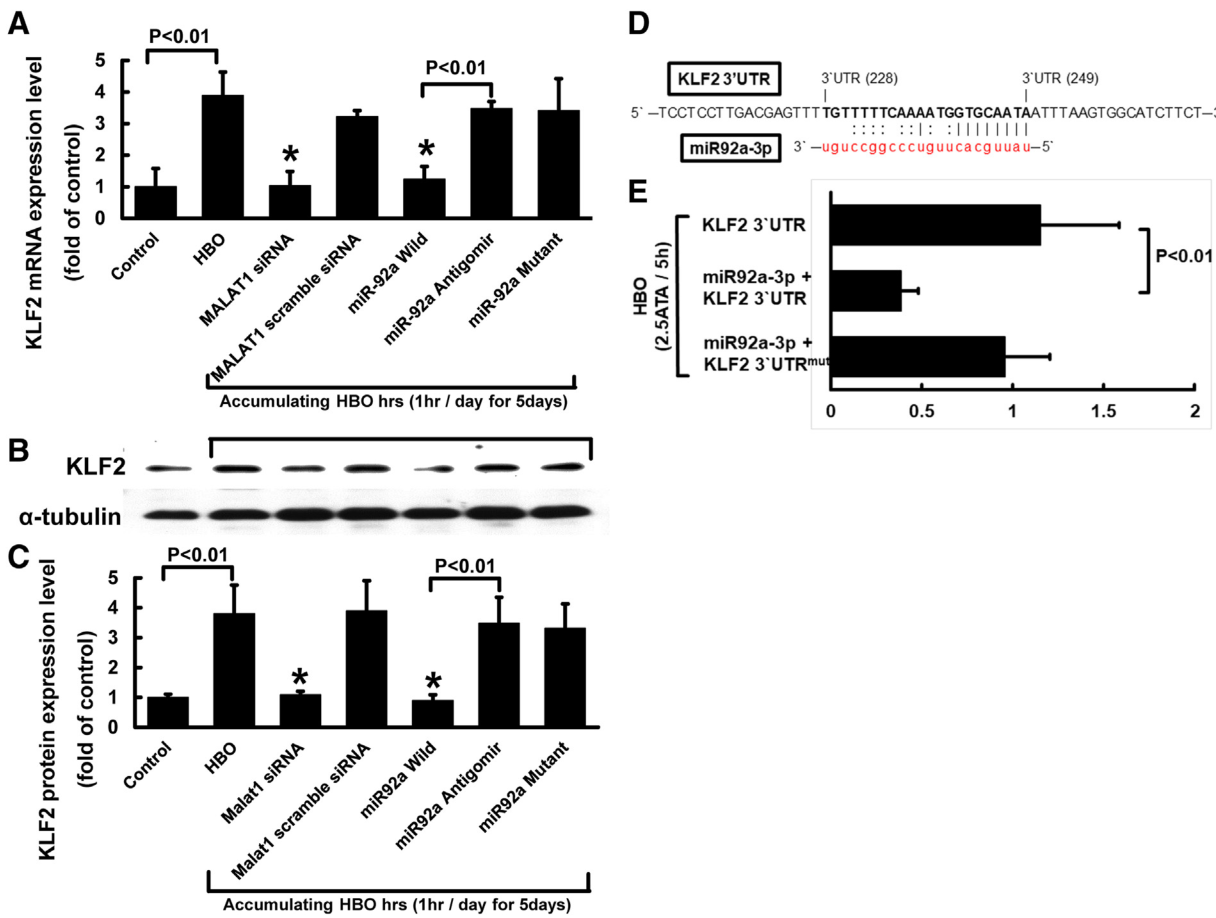

Fig. 3. MALAT1 siRNA and the overexpression of miR-92a inhibited both KLF2 expression in HCAECs under HBO treatment and the effect of miR-92a on KLF2 3′UTR luciferase activity under HBO treatment. A, Quantitative real-time PCR of HCAEC KLF2 mRNA expression under 2.5 ATA at 1 h each day for 5 days. The values from treated HCAECs are expressed as a ratio of normalized values of KLF2 mRNA in the control cells. The Tukey-Kramer comparison test was conducted for statistical analysis. *P < 0.01 vs. HBO; n = 4 per group. B, Representative Western blot. C, Quantitative analysis of KLF2 protein expression under 2.5 ATA at 1 h each day for 5 days. The values from treated HCAEC groups were normalized to match α-tubulin measurements and then expressed as a ratio of normalized value to protein in the control groups. The Tukey–Kramer comparison test was conducted for statistical analysis. *P < 0.01 vs. HBO; n = 4 per group. D, Sequence of the KLF2 3′UTR target site for miR-92a-3p binding, located at KLF2 3′UTR (nucleotide from 228 to 249). E, KLF2 3′UTR luciferase activity under HBO treatment with or without miR-92a-3p. The Tukey–Kramer comparison test was conducted for statistical analysis; n = 4 per group.

HCAEC-derived exosomes. HBO induced MALAT1 expression in a time-dependent and load-dependent manner in HCAECs. Because MALAT1 is regarded as proangiogenic RNA, the increased MALAT1 in HCAECs-derived and HCAEC-derived exosomes may explain the mechanism through which HBO enhances wound healing during neovascularization. Our in vitro study revealed that HBO-induced exosomes from HCAECs could induce the proliferation and tube formation of HCAECs. Our animal model with rat hind-limb ischemia also demonstrated that HBO-induced exosomes from HCAECs improved blood flow to ischemic limbs. The exosomal cargo contained many crucial proteins and microRNAs for the enhancement of angiogenesis [10,19]. Barile et al. identified certain exosome markers, such as TSG101 and Alix, in cardiac progenitor cell-secreted exosomes [20]. In this study, we also discerned the presence of TSG101, which characterizes HCAEC-derived exosomes. Our study is the first to report that HBO can increase endothelial-cell–derived exosomal MALAT1 expression. This finding indicates that exosomes may serve as a novel cell-free approach for therapeutic neovascularization. Exosomes containing MALAT1 might serve as a valuable therapeutic tool for neovascularization through HBO. Indeed, exosomes are stable products that are efficacious after systemic delivery. More significantly, exosomes have high immune tolerability [21].

Just as lncRNA can modulate miR expression, it can also function as miR targets, compete as decoys, or sponge endogenous RNA to prevent the inhibition of mRNA targets [22,23]. In this study, we discovered that MALAT1 shared a unique sequence complementary to miR-92a. MiR-92a plays a vital role in angiogenesis because the forced expression of miR-92a in endothelial cells blocked angiogenesis, and the inhibition of miR-92a enhanced angiogenesis [24,25]. The inhibition of miR-92a could also protect against injury in the form of ischemia/perfusion and prevent endothelial dysfunction and atherosclerosis in animal studies [26,27]. In this study, we demonstrated that HBO significantly decreased miR-92a expression in HCAECs-derived exosomes. Silencing MALAT1 with MALAT1 siRNA could reverse miR-92a expression to the control level. This finding implied that HBO increased MALAT1 expression and that the increased MALAT1 suppressed miR-92a expression. The increased MALAT1 and decreased miR-92a expression in endothelial cells may explain the improvement in angiogenesis after HBO therapy. Indeed, the inhibition of miR92a by antimiR92a has been reported as a therapeutic strategy for promoting skin repair in healing-impaired diabetic mice [28]. Our study also demonstrated that MALAT1 siRNA and miR-92 overexpression could significantly inhibit proliferation and tube formation in HBO-induced HCAECs. Exosomes extracted from HCAECs after HBO treatment also significantly increased cell proliferation and tube formation under typical cultured conditions without HBO treatment. In an animal study, we have demonstrated that HBO and HBO-induced exosomes derived from HCAECs could significantly improve blood flow to ischemic limbs. These results from an in vitro and in vivo study prove that HBO-induced exosomes derived from HCAECs enhanced angiogenesis. Zhang et al. demonstrated that

MALAT1 directly targets vascular endothelial growth factor receptor 2 (VEGFR2) to facilitate angiogenesis [29]. They discovered that MALAT1 silencing significantly reduced tube formation, cell migration, and cell proliferation in cultures from mouse primary skeletal-muscle microvascular endothelial cells. Our results also revealed that MALAT1 derived from HBO-induced exosomes increased VEGFR2 expression in HCAECs (Supplemental Fig. VIII). Our data indicate that HBO may increase exosomal MALAT1 and VEGFR2 to facilitate angiogenesis.

KLF2 has been proven to be a critical mediator for neovascularization [30–32], and Liu et al. demonstrated that KLF2 is the target gene of miR-92a [29]. We observed that miR-92a-3p had a binding site in KLF 3′UTR and that miR-92a could suppress KLF2 luciferase activity by binding to their 3′UTR. This result was consistent with those reported in another study [30]. In the present study, HBO increased KLF2 mRNA and protein expression. MALAT1 siRNA and miR92a inhibited HBO-induced KLF2 mRNA and protein expression. Our study results suggest that HBO upregulates MALAT1 to suppress miR-92 expression and counteracts the inhibitory effect of miR-92a on KLF2 expression in HCAECs.

In summary, our study is the first to report that HBO upregulates MALAT1 to suppress miR-92a expression and counteracts the inhibitory

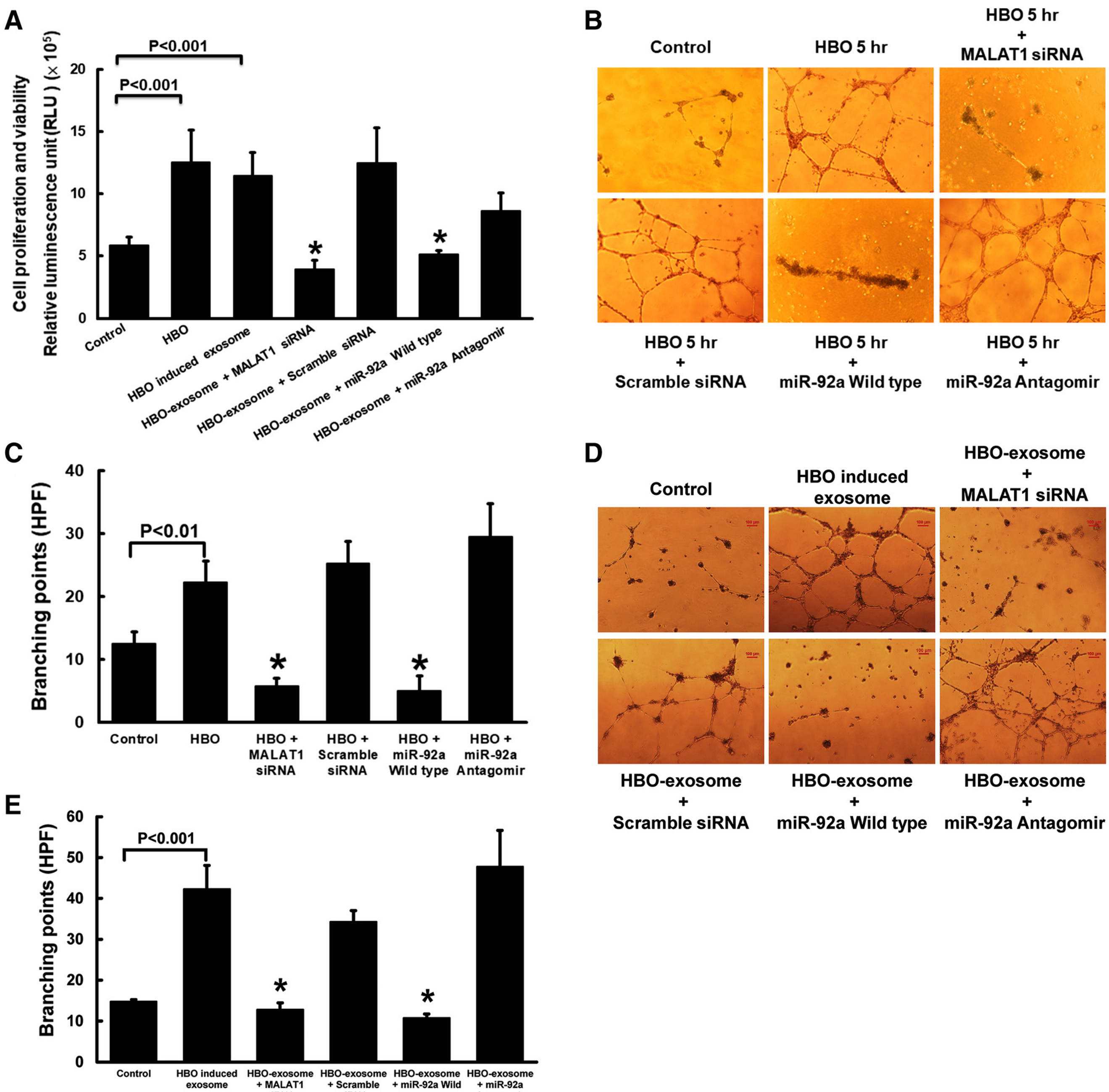

Fig. 4. Effect of HBO and HCAEC-derived exosomes with or without MALAT1 siRNA and miR-92a on the proliferation and capillary-like network formation of HCAECs as well as the effect of HCAEC-derived exosomes and HBO with or without MALAT1 siRNA and miR-92a on ratio of blood flow in hind-limb ischemia. A, Quantitative analysis of HCAEC proliferation and viability. Proliferation and viability assays were performed using the CellTiter-Glo® Luminescent Cell Viability Assay kit. The Tukey–Kramer comparison test was conducted for statistical analysis. *P < 0.001 vs. HBO-induced exosomes; n = 4 per group. B, Representative image of the tube formation of HCAECs under HBO treatment. C, Measurement of quantitative branching points. The Tukey–Kramer comparison test was conducted for statistical analysis. * P < 0.001 vs. HBO alone; n = 4 per group. D, Representative image of the tube formation of HCAECs without HBO treatment. E, Representative image of the tube formation of HCAECs. F, Representative image of Laser Doppler perfusion imaging. G, Quantitative analysis of perfusion recovery with reference to the ratio of blood flow (ischemic/normal hind-limb). The Tukey–Kramer comparison test was conducted for statistical analysis. *P < 0.01 vs. ligation; **P < 0.001 vs. ligation; n = 6 per group.

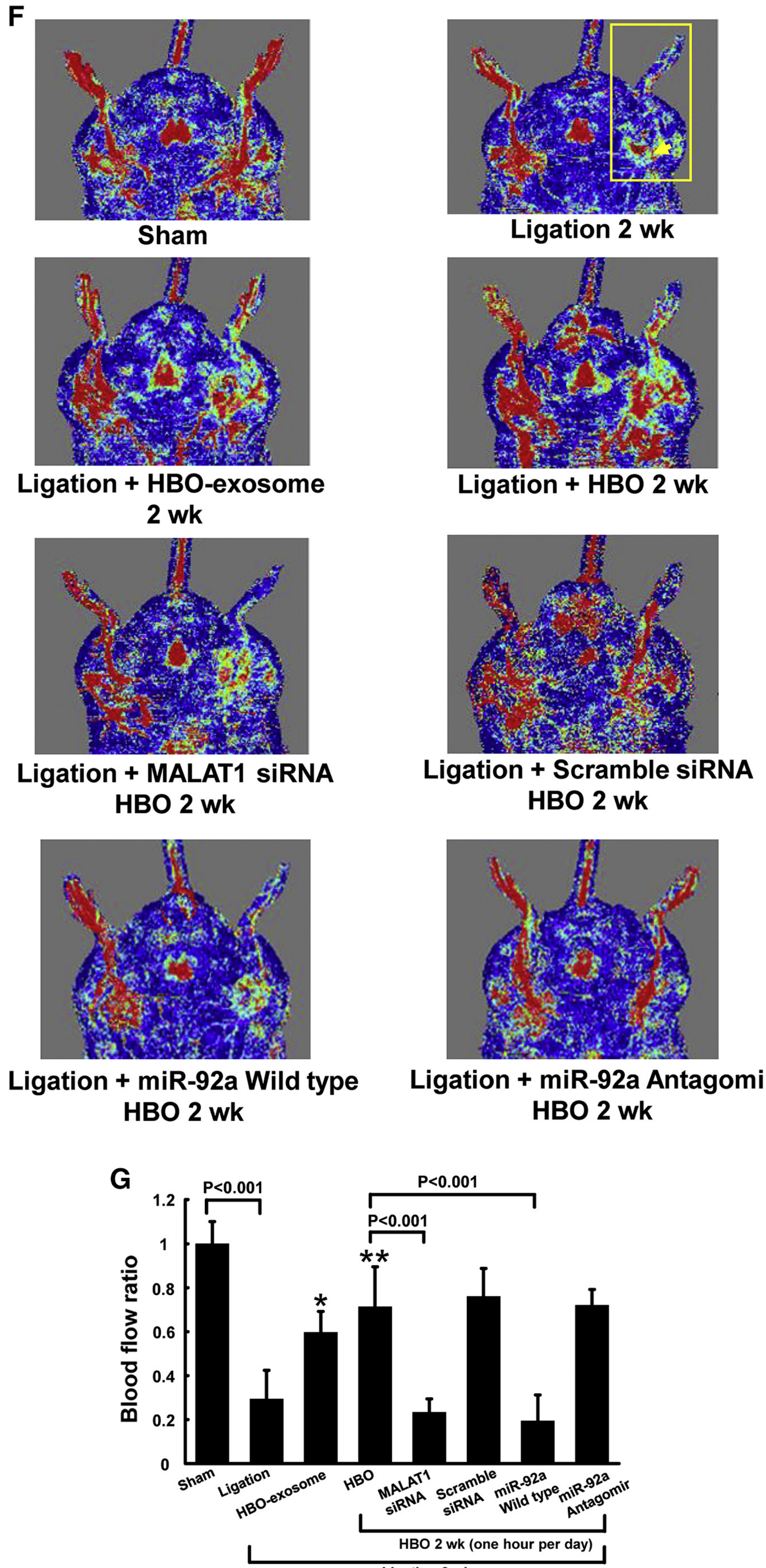

Fig. 4 (*continued*).

effect of miR-92a on KLF2 expression in HCAECs to enhance neovascularization. We proposed a pathway to explain why HCAEC-derived exosomes induced by HBO enhance angiogenesis by upregulating MALAT1 to suppress microRNA-92a expression and counteract the inhibitory effect of miR-92a on KLF2 expression in HCAECs (Graphic Abstract). HBO-induced exosomes derived from HCAECs enhance angiogenesis. Exosomes containing MALAT1 might serve as a valuable therapeutic tool for neovascularization through HBO.

Supplementary data to this article can be found online at https://doi.org/10.1016/j.ijcard.2018.09.118.

Source of funding

The work was supported by grants from the Ministry of Science and Technology, Taiwan (105-2314-B-341-006) and Shin Kong Wu Ho-Su Memorial Hospital (2018SKHADR001), Taipei, Taiwan.

Disclosures

None to declare.

References

[1] P.M. Tibbles, J.S. Edelsberg, Hyperbaric-oxygen therapy, N. Engl. J. Med. 334 (1996) 1642–1648.
[2] B. Tuk, M. Tong, E.M.G. Fijneman, J.M. van Neck, Hyperbaric oxygen therapy to treat diabetes impaired wound healing in rats, PLoS ONE 9 (2014), e108533.
[3] H.M. Kimmel, A. Grant, J. Ditata, The presence of oxygen in wound healing, Wounds 28 (2016) 264–270.
[4] G. Yumun, C. Kahaman, N. Kahaman, U. Yalcinkaya, A. Akcilar, E. Akgui, A.H. Vural, Effects of hyperbaric oxygen therapy combined with platelet-rich plasma on diabetic wounds: an experimental rat model, Arch. Med. Sci. 12 (2016) 1370–1376.
[5] R.A. Boon, N. Jae, L. Holdt, S. Dimmeler, Long noncoding RNAs. From clinical genetics to therapeutic targets? J. Am. Coll. Cardiol. 67 (2016) 1214–1226.
[6] K.M. Michalik, X. You, Y. Manavski, A. Doddaballapur, M. Zornig, T. Braun, D. John, Y. Ponomareva, W. Chen, S. Uchida, R.A. Boon, S. Dimmeler, Long noncoding RNA MALATA regulates endothelial cell function and vessel growth, Circ. Res. 114 (2014) 1389–1397.
[7] J.K. Huang, W.H. Song, Y.B. Huang, H.M. Dong, X.K. Ma, Z.Z. Zhu, R. Zhou, LncRNA-MALAT1 promotes angiogenesis of thyroid cancer by modulating tumor-associated macrophages FGF2 protein secretion, J. Cell. Biochem. 118 (2017) 4821–4830.
[8] X. Li, Y. Song, F. Liu, D. Liu, H. Miao, J. Ren, J. Xu, L. Ding, Y. Hu, Z. Wang, Y. Hou, G. Zhao, Long non-coding RNA MALAT1 promotes proliferation, angiogenesis, and immunosuppressive properties of mesenchymal stem cells by inducing VEGF and IDO, J. Cell. Biochem. 118 (2017) 2780–2791.
[9] L. Barile, T. Moccetti, E. Marban, G. Vassalli, Roles of exosomes in cardioprotection, Eur. Heart J. 38 (2017) 1372–1379.
[10] J.H. Jung, X. Fu, P.C. Yang, Exosomes generated from iPSC-derivatives. New direction for stem cell therapy in human heart diseases, Circ. Res. 120 (2017) 407–417.
[11] L. Barile, V. Lionetti, E. Cervio, M. Matteucci, M. Gherghiceanu, L.M. Popescu, T. Torre, F. Siclari, T. Moccetti, G. Vassalli, Extracellular vesicles from human cardiac progenitor cells inhibit cardiomyocyte apoptosis and improve cardiac function after myocardial infarction, Cardiovasc. Res. 103 (2014) 530–534.
[12] S. Sahoo, E. Klychko, T. Thorne, S. Misener, K.M. Schultz, M. Millay, A. Ito, T. Liu, C. Kamide, H. Agrawal, H. Perlman, G. Qin, R. Kishore, D.W. Losordo, Exosomes from human CD34(+) stem cells mediate their proangiogenic paracrine activity, Circ. Res. 109 (2011) 724–728.
[13] B.W. Wang, C.M. Lin, G.J. Wu, K.G. Shyu, Tumor necrosis factor-α enhances hyperbaric oxygen-induced vistatin expression via JNK pathway in human coronary arterial endothelial cells, J. Biomed. Sci. 18 (2011) 27.
[14] G. Bouachour, P. Cronier, J.P. Gouello, J.L. Toulemonde, A. Talha, P. Alquier, Hyperbaric oxygen therapy in the management of crush injuries: a randomized double-blind placebo-controlled clinical trial, J. Trauma 41 (1996) 333–339.
[15] L. Zhu, J. Liu, S. Ma, S. Zhang, Long noncoding RNA MALAT-1 can predict metastasis and a poor prognosis: a meta-analysis, Pathol. Oncol. Res. 21 (2015) 1259–1264.
[16] S. Uchida, S. Dimmeler, Long noncoding RNAs in cardiovascular diseases, Circ. Res. 116 (2015) 737–750.
[17] J.Y. Sun, Z.W. Zhao, W.M. Li, G. Yang, P.Y. Jing, P. Li, H.Z. Dang, Z. Chen, Y.A. Zhou, X.F. Li, Knockdown of MALAT1 expression inhibits HUVEC proliferation by upregulation of miR-320a and downregulation of FOXM1 expression, Oncotarget 8 (2017) 61499–61509.
[18] M. Zhang, H. Gu, W. Xu, X. Zhou, Down-regulation of lncRNA MALAT1 reduces cardiomyocyte apoptosis and improves left ventricular function in diabetic rats, Int. J. Cardiol. 203 (2016) 214–216.
[19] B.W. van Balkom, O.G. de Jong, M. Smits, J. Brummelman, K. den Quden, P.M. de Bree, M.A. van Eijndhoven, D.M. Pegtel, W. Stoorovogel, T. Wurdinger, M.C. Verhaar, Endothelial cells require miR-214 to secrete exosomes that suppress senescence and induce angiogenesis in human and mouse endothelial cells, Blood 122 (3997–4006) (2013) S1–S5.
[20] L. Barile, E. Cervio, V. Lionetti, G. Milano, A. Ciullo, V. Biemmi, S. Bolis, C. Altomare, M. Matteucci, D.D. Silvestre, F. Bambilla, T.E. Fertig, T. Torre, S. Demertzis, P. Mauri, T. Moccetti, G. Vassalli, Cardioprotection by cardiac progenitor cell-secreted exosomes: role of pregnancy-associated plasma protein-A, Cardiovasc. Res. 114 (2018) 992–1005.
[21] E. Marban, The secret life of exosomes. What bees can teach us about next-generation therapeutics, J. Am. Coll. Cardiol. 71 (2018) 193–200.
[22] K.N. Smith, J. Starmer, S.C. Miller, P. Sethupathy, T. Magnuson, Long noncoding RNA moderates microRNA activity to maintain self-renewal in embryonic stem cells, Stem Cell Rep. 9 (2017) 108–121.
[23] M.S. Ebert, P.A. Sharp, Emerging roles for natural mircoRNA sponges, Curr. Biol. 20 (2010) R858–R861.
[24] A. Bonauer, G. Carmona, M. Iwasaki, M. Mione, M. Koyanagi, A. Fischer, J. Burchfield, H. Fox, C. Doebele, K. Ohtani, E. Chavakis, M. Potente, M. Tjwa, C. Urbich, A.M. Zeiher, S. Dimmeler, MicroRNA-92a controls angiogenesis and functional recovery of ischemic tissue in mice, Science 324 (2009) 1710–1713.
[25] K. Murata, H. Ito, H. Yoshitomi, K. Yamamoto, A. Fukuda, J. Yoshikawa, M. Furu, M. Ishikawa, H. Shibuya, S. Matsuda, Inhibition of miR-92a enhances fracture healing via promoting angiogenesis in a model of stabilized fracture in young mice, J. Bone Miner. Res. 29 (2014) 316–326.
[26] R. Hinkel, D. Penzkofer, S. Zuhlke, A. Fischer, W. Husada, Q.F. Xu, E. Baloch, E. van Rooij, A.M. Zeiher, C. Kupatt, S. Dimmeler, Inhibition of micrRNA-92a protects against ischemia/reperfusion injury in a large-animal model, Circulation 128 (2013) 1066–1075.
[27] X. Loyer, S. Potteaux, A.-C. Vion, C.L. Guerin, S. Boulkroum, P.-E. Rautou, B. Ramkhelawon, B. Esposito, M. Dalloz, J.-L. Paul, P. Julia, L. Maccario, C.M. Boulanger, Z. Mallat, A. Tedgui, Inhibition of microRNA-92a prevents endothelial dysfunction and atherosclerosis in mice, Circ. Res. 114 (2014) 434–443.
[28] T. Lucas, F. Schafer, P. Muller, S.A. Eming, A. Heckel, S. Dimmeler, Light-inducible antimiR-92a as a therapeutic strategy to promote skin repair in healing-impaired diabetic mice, Nat. Commun. 8 (2017), 15162. https://doi.org/10.1038/ncomms15162.
[29] X. Zhang, X. Tang, M.H. Hamblin, K.J. Yin, Long non-coding RNA Malat1 regulates angiogenesis in hind-limb ischemia, Int. J. Mol. Sci. 19 (2018), E1723.
[30] H. Liu, G. Li, W. Zhao, Y. Hu, Inhibition of miR-92a may protect endothelial cells after acute myocardial infarction in the rats: role of KLF2/4, Med. Sci. Monit. 22 (2016) 2451–2462.
[31] M. Renz, C. Otten, E. Faurobert, F. Rudolph, Y. Zhu, G. Boulday, J. Duchene, M. Mickoleit, A.C. Dietrich, C. Ramspacher, E. Steed, S. Manet-Dupé, A. Benz, D. Hassel, J. Vermot, J. Huisken, E. Tournier-Lasserve, U. Felbor, U. Sure, C. Albiges-Rizo, S. Abdelilah-Seyfried, Regulation of β1 integrin-Klf2-mediated angiogenesis by CCM proteins, Dev. Cell 32 (2015) 181–190.
[32] R.A. Boon, C. Urbich, A. Fischer, R.D. Fontijn, F.H. Seeger, M. Koyanag, A.J.G. Horrevoets, S. Dimmeler, Kruppel-like factor 2 improves neovascularization capacity of aged proangiogenic cells, Eur. Heart J. 32 (2011) 371–377.